Journal of Applied Geophysics 82 (2012) 171–183

Contents lists available at SciVerse ScienceDirect

Journal of Applied Geophysics

journal homepage: www.elsevier.com/locate/jappgeo

# Fast-decaying inductively induced polarization in frozen ground: A synthesis of results and models

N.O. Kozhevnikov, E.Yu. Antonov *

*Institute of Petroleum Geology and Geophysics, Siberian Branch of the Russian Academy of Sciences, 3, prosp. Koptyuga, Novosibirsk 630090, Russia*

ARTICLE INFO

*Article history:*
Received 16 July 2011
Accepted 16 March 2012
Available online 28 March 2012

*Keywords:*
TEM surveys
Induced polarization
Frozen ground
Low-frequency dielectric permittivity
Electrochemical polarization
Surface conductance

ABSTRACT

Many TEM data from Yakutia and other areas of widespread permafrost bear a manifestation of the induced polarization (IP) effect. The distinguishing feature of this effect is the distortion in the monotony, sign reversals included TEM voltage responses in the time range from a few tens to a few hundreds of microseconds. According to the inversion of TEM responses in terms of the Cole–Cole conductivity model, the IP effects are produced by fast decaying polarization in the upper 100 m of frozen ground. Shallow frozen rocks exhibit the chargeability $m$ in the range 0.2 to 0.85, mostly within 0.2–0.5, the relaxation time $\tau$ from 35 to 250 μs (50 to 100 μs on average). As for the exponent $c$, it is usually in the range 0.8 to 1, which is evidence of a narrow range of the relaxation times. Conversion of chargeability into low-frequency dielectric permittivity gives values of the order of tens or a few hundreds of thousands. These very high permittivities cannot be explained by dielectric relaxation of ice inclusions and/or interfacial polarization. A more likely reason is electrochemical polarization of the films of unfrozen water on the mineral grain and ice inclusion surfaces. It is convenient to interpret the electrochemical polarization effects in terms of frequency-dependent surface conductivity controlled by the surface-to-volume ratio. For an unfrozen wet rock the surface conductivity is small compared to the bulk conductivity of the pore water. However, upon freezing the pore water, the surface conductivity becomes dominant which results in the manifestation of IP phenomena. An additional reason why freezing of a wet porous rock is favorable for the manifestation of IP effects in TEM data is that the relative contribution of eddy currents becomes less than that of polarization ones.



## 1. Introduction

TEM responses measured over permafrost areas (Yakutia, Canada, Alaska, etc.) are often nonmonotonous or even exhibit sign reversals caused by the fast-decaying induced polarization (IP) of rocks (Kozhevnikov and Antonov, 2006; Krylov and Bobrov, 1998, 2002; Molchanov and Sidorov, 1985; Sidorov, 1985, 1987; Smith and Klein, 1996; Stognii, 2008; Stognii and Korotkov, 2010; Vanchugov and Kozhevnikov, 1998; Walker and Kawasaki, 1988). The IP effects show up in the frequency domain as frequency dependence of conductivity and/or dielectric permittivity of the ground. It should be recalled that it was G. R. Olhoeft (1978) who first measured conductivity and dielectric permittivity of permafrost over a wide frequency range and drew attention to their strong frequency dependence.

IP-affected TEM data were reported not only from northern territories, but it is in permafrost areas that the effects are so persistent. For instance, TEM surveys in Yakutia yielded thousands or maybe tens of thousands IP-effected TEM responses. There are reasons to attribute the fast-decaying polarizability of frozen rocks in Yakutia to ion-conductance mechanisms rather than to the electrode polarization due to the presence of electron-conductive mineral grains (Kozhevnikov and Antonov, 2006, 2009b, 2010; Olenchenko et al., 2008; Stognii, 2008).

Explicit evidence that the same rocks in situ produce IP-affected TEM responses when they are frozen but are not polarizable in the unfrozen state was obtained in a specially designed field experiment in the vicinity of Taksimo Village, northern Buryatia (Kozhevnikov and Antonov, 2006; Kozhevnikov et al., 1995). The measurements were made on sand that showed low polarization when unfrozen but gave significant manifestation of IP in areas where it was known to be frozen. The inference that the distortion of TEM signals resulted from induced polarization was supported by early-time IP measurements with a galvanic system.

IP-affected TEM responses have been observed in Yakutia since the 1970s, but the interpretation of these TEM data was precluded for a long time by the lack of the appropriate tools. Estimating the chargeability of rocks in the area, where TEM surveys are employed for kimberlite exploration and mapping, became possible as the respective modeling software was designed (Kozhevnikov and Antonov, 2006, 2008; Stognii, 2008).

Obviously the next step in studying inductively induced polarization in permafrost terrains would be to interpret the obtained polarization parameters in terms of rock physics, i.e., to explain *why* the IP effects appear when a rock freezes up.

* Corresponding author.
*E-mail address:* antonovemf@yandex.ru (E.Y. Antonov).

0926-9851/$ – see front matter © 2012 Elsevier B.V. All rights reserved.
doi:10.1016/j.jappgeo.2012.03.008

## 2. Simplified physics of the inductive ip

The best way to illustrate the inductively induced polarization phenomenon is with an example of a weakly polarizable conductive ground (Flis et al., 1989; Kozhevnikov and Antonov, 2009a). Fig. 1 shows an ungrounded loop (1) with steady current in it. The loop lies on a ground with the dc conductivity $\sigma_0$. As the transmitter current is turned off at the time $t=0$, the primary magnetic field $\boldsymbol{B}_1$ instantaneously goes to zero inducing in the ground eddy currents with their field $\boldsymbol{B}_2$ which, at early times, is the same as $\boldsymbol{B}_1$. The eddy currents within some rock volume 2, consist of free charges 3 (ions) that move under the applied vortex electric field $\boldsymbol{E}$. According to Ohm's law, the eddy current density $\boldsymbol{j}_{\text{cond}}$ is controlled by the conductivity $\sigma$:

$$E = j_{\text{cond}}/\sigma. \tag{1}$$

Assume that a small "inclusion" (4) in volume 2 contains some bound charges, i.e., is polarizable. If its chargeability is low, as we have assumed, the conduction current distribution and, correspondingly, the field $\boldsymbol{E}$ remain governed by the conductivity $\sigma_0$. The "inclusion" that bears bound charges polarizes in response to the applied electric field $\boldsymbol{E}$. In the case being considered, the effect of $\boldsymbol{E}$ is to induce the polarization (or *displacement*) currents $\boldsymbol{I}_{\text{pol}}$ in 4, $\boldsymbol{I}_{\text{pol}}$ being proportional to the rate of the $\boldsymbol{E}$ decay. Like the eddy currents, the polarization currents induce a magnetic field which contributes to the total TEM response.

At early times, the polarization currents have the same direction as the vortex currents (Fig. 1b), but then $\boldsymbol{I}_{\text{pol}}$ comes to zero as the polarization process stops at some time when further separation of the bound charges is no longer possible (Fig. 1c).

Once the eddy currents become orders of magnitude lower as a result of heat loss, there is no longer electric field forcing the bound charges to separate (Fig. 1d) and they return to their equilibrium distribution, i.e., there arise polarization currents opposite in direction to the initial one (Fig. 1b). At that stage, the magnetic field of polarization currents has the polarity opposite to that resulting from the "normal" eddy currents.

The "inclusions" with bound charges may represent various objects: electron-conducting mineral grains in ion-conducting rock, or systems of electrolyte-filled pores of different sizes, or electrical double layers on pore walls and around clay particles, or ice inclusions, etc.

Note that the IP contribution to the TEM response of conductive, polarizable ground or a polarizable object depends on the relative decay rates of the conduction and polarization currents. If the polarization currents decay faster than the conduction ones, the former can show up only as a small perturbation against the latter. Otherwise, the conduction currents decay faster but this short time is *enough* for a system of slowly decaying polarization currents to form under the action of vortex electric field $\boldsymbol{E}$. After the eddy currents have disappeared, the polarization current at any one point of the ground flows in the direction opposite to the direction that eddy current had at the same point. Thus, the polarization currents make a "mirror image" of the early-time conduction currents (Smith et al., 1988).

## 3. Phenomenological models of conductivity and dielectric dispersion in rocks

Forward modeling and inversion of TEM responses is often made first in the frequency domain, and the results are transformed then into the time domain. Fast-decaying induced polarization is taken into account via the Cole–Cole complex resistivity model which frequency-dependent conductivity $\sigma^*(\omega)$ (Flis et al., 1989; Lee, 1981; Wait, 1982):

$$\sigma^*(\omega) = \sigma_0 \frac{1+(j\omega\tau)^c}{1+(1-m)(j\omega\tau)^c}, \tag{2}$$

where $j=\sqrt{-1}$; $\omega$ is the angular frequency, in $s^{-1}$; $\sigma_0$ is the dc conductivity, in S/m; $m$ is the chargeability, $(0 \le m < 1)$; $\tau$ is the IP relaxation time constant, in s; $c$ is the exponent $(0 \le c \le 1$, 1 and 0 corresponding,

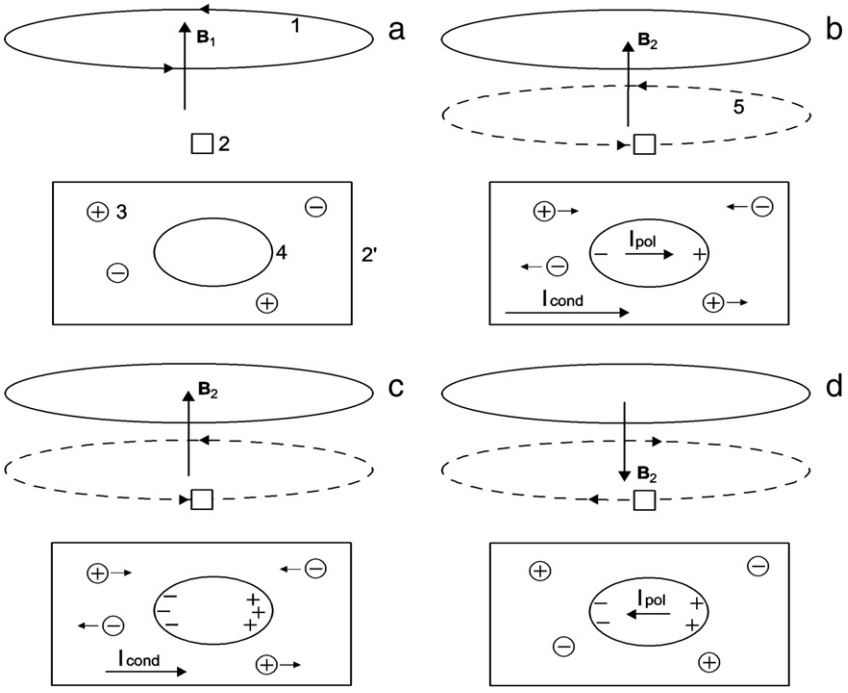


**Fig.1.** Inductively induced electrical polarization in rocks. Prior to the turn-off of transmitter current, free and bound charges are distributed evenly and current in the ground is zero (a). As the current in transmitter loop is turned off, and some time after that, both free and bound charges move making a positively directed current flowing in ground (b). The bound charges stop moving at some time, and the polarization current becomes zero (c). At late times, the vortex electric field decreases and becomes unable of maintaining the separating of bound charges which, returning to the equilibrium, produce polarization current flowing in the direction opposite to that shown in panel b (d). 1 is the transmitter loop; 2 is a small volume of the medium; 2′ is the same volume, enlarged; 3 is a free charge; 4 is a polarizable inclusion; 5 is the current line. $\mathbf{B}_1$ is the primary magnetic field; $\mathbf{B}_2$ is the secondary magnetic field; $\mathbf{I}_{\text{cond}}$ is the conduction current; $\mathbf{I}_{\text{pol}}$ is the polarization current.

respectively, to a single relaxation time and to an infinitely broad uniform distribution of relaxation times). It should be recalled that it were Pelton et al. (1978) who first proposed the Cole–Cole resistivity model for geophysical application.

The chargeability $m$ can be expressed as

$$m = \frac{\sigma_\infty - \sigma_0}{\sigma_\infty}, \tag{3}$$

where $\sigma_0$ is the conductivity measured at frequencies much below the relaxation frequency $f_\theta = (2\pi\tau)^{-1}$ and $\sigma_\infty$ is the conductivity at a frequencies much higher than $f_\theta$.

When using Eq. (2) to account for dependence of rock electrical properties on frequency one usually assumes that the dielectric permittivity does not depend on frequency and causes no influence on the measured signals. On the other hand, as we showed earlier (Kozhevnikov and Antonov, 2006; Kozhevnikov and Artemenko, 2004), using Eq. (2) at the frequencies corresponding to spectra of the TEM responses is equivalent to an alternative model which combines $\sigma_0$ and complex and frequency-dependent dielectric permittivity. The Cole–Cole complex dielectric permittivity is (Frolov, 1998; Hippel, 1954)

$$\varepsilon^*(\omega) = \varepsilon_0\left(\varepsilon_\infty + \frac{\varepsilon_s - \varepsilon_\infty}{1 + (j\omega\tau)^c}\right), \tag{4}$$

where $\varepsilon_0$ is the free-space dielectric constant ($8.854 \cdot 10^{-12}$ F/m); $\varepsilon_s$, $\varepsilon_\infty$ are the relative static and dynamic permittivities, respectively; $\tau$ is the time constant of dielectric relaxation, in seconds, and $c$ is the exponent. Fast-decaying polarization is described in this way in laboratory dielectric measurements on frozen ground samples (Bittelli et al., 2004; Frolov, 1998). The case of $c = 1$ corresponds to the Debye relaxation.

The conductivity $\sigma^*(\omega)$ of a rock with the frequency-independent dc conductivity $\sigma_0$ and the complex permittivity given by Eq. (4) is

$$\sigma^*(\omega) = \sigma_0 + j\omega\varepsilon_0\left[\varepsilon_\infty + \frac{\varepsilon_s - \varepsilon_\infty}{1 + (j\omega\tau)^c}\right]. \tag{5}$$

In model (2), it is the chargeability $m$ that measures the capability of a medium to polarize under the applied electric field while in models (4) and (5) this is the difference $\Delta\varepsilon$ between the relative static and dynamic permittivities ($\Delta\varepsilon = \varepsilon_s - \varepsilon_\infty$) called the *dielectric increment* (Chelidze et al., 1999). This parameter is free from the effects of the dc conductivity, while the chargeability $m$ is subject to both polarization and conductivity controls (Lesmes and Frye, 2001; Lesmes, 2005). Normally $\varepsilon_\infty \ll \varepsilon_s$, $\Delta\varepsilon \cong \varepsilon_s$, therefore, $\varepsilon_s$ can be used as a measure of the dielectric dispersion.

In the case of the Debye-like relaxation a simple formula can be derived relating the chargeability and the dielectric increment. Assuming in Eq. (5) $c = 1$ and separating $\sigma^*$ into real $\sigma'$ and imaginary $\sigma''$ parts results in

$$\mathrm{Re}\sigma^* = \sigma' = \sigma_0 + \frac{\omega^2\varepsilon_0\tau(\varepsilon_s - \varepsilon_\infty)}{1 + \omega^2\tau^2}, \tag{6}$$

$$\mathrm{Im}\sigma^* = \sigma'' = \omega\varepsilon_0\left(\varepsilon_\infty + \frac{\varepsilon_s - \varepsilon_\infty}{1 + \omega^2\tau^2}\right). \tag{7}$$

Usually, at frequencies below 100 kHz $\sigma''(\omega) \ll \sigma'(\omega)$, so we can assume $\sigma^* \cong \sigma'$, and Eq. (5) may be rewritten as

$$\sigma^*(\omega) \cong \mathrm{Re}\sigma^* = \sigma_0 + \frac{\omega^2\varepsilon_0\tau(\varepsilon_s - \varepsilon_\infty)}{1 + \omega^2\tau^2}. \tag{8}$$

Normally upper frequency limit in the spectra of signals measured in inductive prospecting methods does not exceed few tens of kHz, so the frequencies above 100 kHz can be considered as practically infinitely high for determining $\sigma_\infty$. Since at high frequencies $\omega^2\tau^2 \gg 1$, from Eq. (8) we obtain $\sigma_\infty = \sigma_0 + \varepsilon_0(\varepsilon_s - \varepsilon_\infty)/\tau$. Substituting the $\sigma_0$ and $\sigma_\infty$ into Eq. (3) gives the formula for the chargeability of geological materials with frequency-independent conductivity $\sigma_0$ and dielectric permittivity described by the Debye relaxation model (Kozhevnikov and Antonov, 2006; Kozhevnikov and Artemenko, 2004):

$$m = \left[1 + \frac{\sigma_0\tau}{\varepsilon_0(\varepsilon_s - \varepsilon_\infty)}\right]^{-1}. \tag{9}$$

This means that writing the polarizability via the frequency-independent conductivity $\sigma_0$ and the complex dielectric permittivity $\varepsilon^*(\omega)$ following Eq. (3) at $c = 1$ is equivalent to using the complex frequency-dependent conductivity $\sigma^*(\omega)$ given by Eq. (1) with $\sigma_0$, $c = 1$, and the chargeability $m$ according to Eq. (8).

## 4. Results: inversion of tem data from cold regions

The inversion of TEM responses consisted in fitting a 1D earth model to measured data. The IP effects were allowed for by using complex frequency-dependent conductivity of Eq. (1). For more details of the procedure and the results see Kozhevnikov and Antonov (2006, 2008, 2009a, b; 2010), Stognii (2008), and Stognii and Korotkov (2010). Below we discuss examples of TEM responses measured in cold regions and affected by the fast-decaying IP.

### 4.1. Kimberlite fields, Western Yakutia

The transients in Fig. 2 were measured at two sites in the vicinity of Mirny in Western Yakutia (Kozhevnikov and Antonov, 2008). The local geology consists of thin Quaternary unconsolidated sediments overlying Jurassic sand and clay underlain by Lower Paleozoic terrigenous-carbonate sediments. The measurements were performed with 100 m × 100 m (Fig. 2a) and 50 m × 50 m (Fig. 2b) coincident-loop arrays. A commercially available instrument TSIKL-5 (*Elta-Geo* Novosibirsk) was used to produce and measure transients.

The small triangles and the diamonds in Fig. 2 are the measured TEM responses and the solid lines are the ones derived by inversion in terms of a 1D polarizable earth model. The transients obviously are affected by fast-decaying IP. The inverted models on the right-

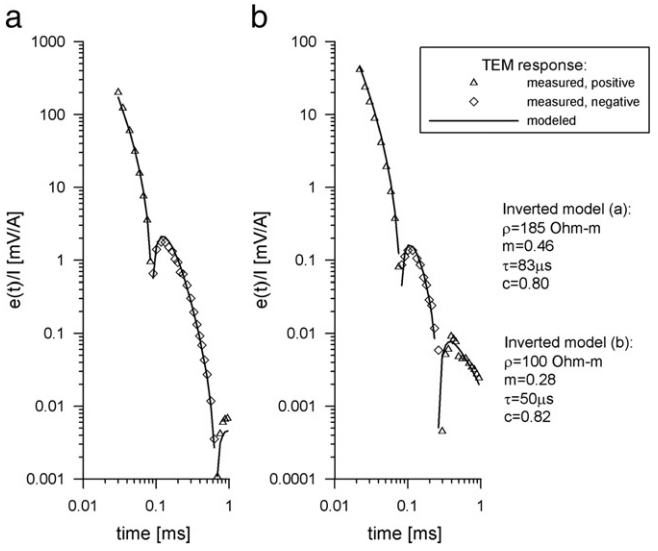


**Fig. 2.** Inversion of TEM responses measured in West Yakutia, Russia: (a) vicinity of Mirny city, near a kimberlite pipe, 100 m by 100 m coincident-loop configuration; (b) vicinity of Mirny city, near a quarry, 50 m by 50 m coincident-loop configuration (Kozhevnikov and Antonov, 2008).

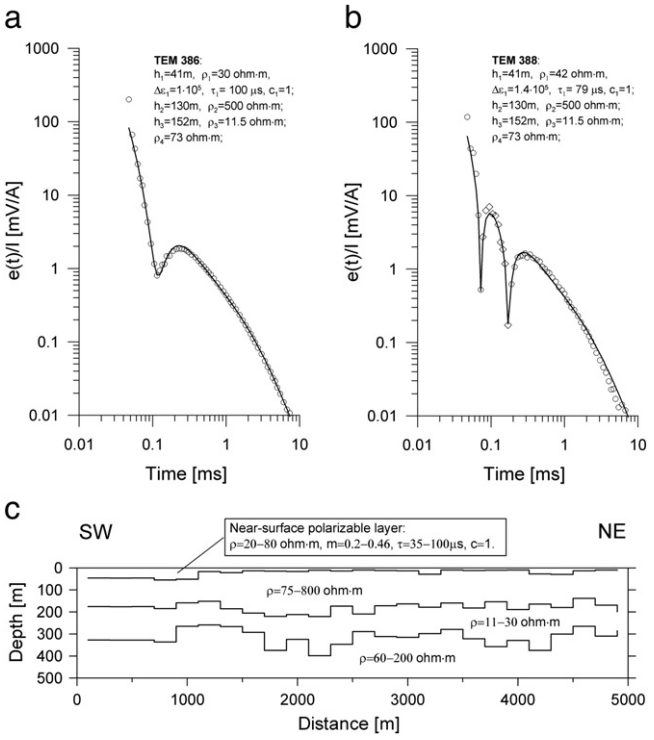


**Fig. 3.** Inversion of TEM data measured on the Nakyn kimberlite field in Western Yakutiya, Russia: a) measured and modeled TEM responses exhibiting distortion in the monotony without polarity change; b) measured and modeled TEM responses exhibiting double polarity change; c) resistivity and chargeability section assembled from 1D inversion results. Open circles and diamonds in (a) and (b) indicate positive and negative measured data, respectively, and solid line indicates the inversion data (Kozhevnikov and Antonov, 2006).

hand panel of the figure correspond to a uniform polarizable earth with $\rho = 100–185\ \Omega\cdot m$, $m = 0.28–0.46$, $\tau = 50–83\ \mu s$, $c = 0.8$.

The other example (Fig. 3) is from the Nakyn kimberlite field in Western Yakutia (Kozhevnikov and Antonov, 2006). The near-surface geology comprises Jurassic sand and clay, from a few meters to 100 m thick, lying over Lower Paleozoic carbonate and carbonate-clay rocks which host kimberlites. The TEM responses were measured in the time range from a few tens of microseconds to ten milliseconds with a *Tsikl-Mikro* instrument using a central-loop configuration with the loop sizes 200 m × 200 m (transmitter) and 100 m × 100 m (receiver). Altogether 25 TEM soundings were taken at every 200 m along the profile.

Almost all transients are IP affected. Panels *a* and *b* above are the measured and computed TEM responses and 1D earth models obtained through the inversion. The panel below (c) is a geoelectrical section based on 1D inversion of all TEM responses measured along the profile.

The geoelectrical section consists of four layers. The second layer (from above) encompasses Jurassic and Lower Paleozoic terrigenous-carbonate rocks. Its resistivity varies from 75 to 800 Ω·m and the thickness is from 110 to 210 m. The third layer, from 80 to 210 m thick, with the resistivity 11 to 30 Ω·m, is a porous formation saturated with saline water. Although the depth to the frozen ground base is here about 400 m, the interstitial water does not freeze because of its high salinity, which is the reason why the third layer resistivity is low. The top of the layer was recognized during TEM surveys over the Nyurba kimberlite pipe and its vicinities (Vanchugov and Kozhevnikov, 1998). The base of the section is 60 to 200 Ω·m Lower Paleozoic terrigenous-carbonate rocks.

The uppermost layer, with its thickness 10 to 50 m and resistivity from 20 to 80 Ω·m, is polarizable. Its chargeability $m$ varies from 0.2 to 0.46, the relaxation time $\tau$ is from 35 to 100 μs, and the exponent is $c = 1$ for all responses. The layer consists of frozen Quaternary and upper Jurassic sediments. According to (Klimovsky and Gotovtsev, 1994) the ice content in the Quaternary sediments of the Yakutia diamond province is high (from 10 to 50 vol.%). Some layers of the Jurassic sedimentary section lying under the Quaternary sediments contain clay material.

The inversion of the Yakutia TEM data showed the Cole–Cole parameters listed in Table 1: the chargeability $m$ in the range 0.2 to 0.85, most often within 0.2–0.5; the time constant $\tau$ from 35 to 250 μs, averaging about 100 μs; and the exponent $c$ about 0.8 to 1, little variable unlike $m$ and $\tau$.

The fact that in most cases $c \cong 1$ indicates a narrow range of relaxation times and makes the polarization process actually fitting the Debye model. Thus the IP process can be approximated by an exponential decay with the time constant $\tau$, which allows one to estimate $\Delta\varepsilon$ using Eq. (9) (see the lower row in Table 1 for the respective values).

### 4.2. An Arctic glacier

One of the hypotheses accounting for the fast-decaying IP in frozen ground attributes this phenomenon to dielectric relaxation in ice inherent in frozen rocks (Kozhevnikov et al., 1995; Stognii, 2008; Stognii and Korotkov, 2010). The electric properties of mono- and polycrystalline ice depending on the water salinity, frequency and temperature were investigated in exhaustive laboratory experiments on natural and synthetic samples (Frolov, 1998). As for the electric properties of in situ ice, dc or low-frequency conductivity and high-frequency dielectric permittivity were extensively studied, respectively, by resistivity methods and GPR soundings. The frequency dependence of conductivity and/or permittivity of in situ ice has been poorly explored, and the literature is limited (Reynolds, 1985). Quite often, however, the measured physical parameters of rocks depend on the effective volume of samples. Among geophysicists this phenomenon is known as a "scaling problem" (Ogilvi, 1990). In connection with this it would be interesting to measure the transient responses of in situ massive ice, say, in a glacier.

A full-size field experiment in areas of natural glaciers being very costly and hard to organize, any reports on the subject are of particular value. In this respect we paid attention to a publication on a TEM sounding data measured in 1984 on an Arctic glacier (Vostretsov et al., 1985). The thickness of freshwater ice at the site was 500 m, and drilling was to a depth of 400 m. The ice temperature within that depth range was about −10 °C, the total salinity was 20 mg/L.

The measurements were performed using a *Kaskad* instrument (Sidorov, 1985). The 25 m by 25 m, 50 m by 50 m, 100 m by 100 m, and 200 m by 200 m square coincident loops were laid in a way that their centers were at the same point.

The figure with measured transients from (Vostretsov et al., 1985) was digitized to obtain a dataset suitable for the inversion. See Fig. 4

**Table 1**
Parameters of the near-surface polarizable layer found by inversion of TEM responses measured in Western Yakutia (Kozhevnikov and Antonov, 2006, 2008; Stognii, 2008).

| Site | XXIII CPSU congress kimberlite pipe | Trap (basalt) quarry, vicinity of Mirny | Nakyn kimberlite field | Taezhnaya kimberlite pipe | Upper Chuonalyr | D'yakhtar |
|---|---|---|---|---|---|---|
| $\rho$, Ω·m | 185 | 100 | 20–80 | 200 | 600 | 190 |
| $m$ | 0.46 | 0.28 | 0.20–0.46 | 0.55 | 0.70–0.85 | 0.59 |
| $\tau$, μs | 83 | 50 | 35–100 | 110 | 170–250 | 93 |
| $c$ | 0.80 | 0.82 | 1 | 0.85 | 0.80–0.90 | 0.9 |
| $h$, m | ≤100 | ≤100 | 10–50 | 15 | ≤10 | 45 |
| $\Delta\varepsilon$ | $4.3 \cdot 10^4$ | $2.2 \cdot 10^4$ | $1.5 \cdot 10^4$–$2 \cdot 10^5$ | $7.6 \cdot 10^4$ | $7.5 \cdot 10^4$–$2.7 \cdot 10^5$ | $8 \cdot 10^4$ |

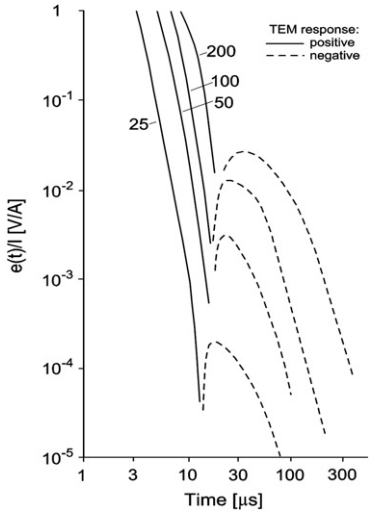


**Fig. 4.** TEM responses measured with coincident-loop configurations on an Arctic glacier (Vostretsov et al., 1985). The curves are labeled according to loop side length (m).

for the TEM responses derived from those data. All TEM responses show a sign reversal: the signal has a positive polarity at early times, then the sign changes, the voltage goes through minimum and then there follows decrease in the signal magnitude. This is an unambiguous evidence of IP effects since the above TEM responses were measured with coincident loop configuration: as was shown by Weidelt (1982), for any physically reasonable frequency-independent distribution of electrical conductivity the coincident loop voltage response is of one sign only.

As the measurements on the glacier were taken at the same point by loops of different sizes, we applied single and joint inversion of the TEM data using the *TEM-IP* computer program (Antonov et al., 2010). In the case of joint inversion minimized was the error functional which included the different loop size responses (Kozhevnikov and Antonov, 2008, 2009a, 2009b, 2010). The results of the single and joint inversion for different loop configurations along with rms errors are given in Table 2. The rms errors were calculated as

$$\mathrm{rms} = \left\{ \frac{1}{N-1} \sum_{i=1}^{N} \left[ \frac{e^{\mathrm{meas}}(t_i) - F_{\mathbf{p}}(t_i)}{e^{\mathrm{meas}}(t_i)} \right]^2 \right\}^{1/2}, \qquad (10)$$

where $t_i$ is the $i$-th time delay; $N$ is the total number of time delays; $e^{\mathrm{meas}}(t_i)$ is the transient emf measured at the $i$-th time delay; $F_{\mathrm{p}}$ is the forward operator.

In all cases, the fitting resulted in a two-layer model with a polarizable layer above and a non-polarizable basement below. The polarizable layer had the following parameters: average thickness is 120 m, resistivity $\rho_1 = 2 \cdot 10^3\ \Omega\cdot$m; average chargeability $m_1 = 0.36$; time constant $\tau_1 = 37$ μs; exponent $c_1 = 0.9$. The resistivity of the basement, $\rho_2$, was found to be of about $3.5 \cdot 10^3\ \Omega\cdot$m.

Fig. 5 illustrates the quality of single inversion for each loop configuration. In this case, the relative rms was 9–33%. Joint inversion gave a greater misfit between the measured and computed data (Fig. 6): the rms reached 45 to 70%.

The Debye-type relaxation of the process with $c \cong 1$ indicates a single exponentially decreasing signal. This enables the use of Eq. (9) to find $\Delta\varepsilon_1$. The respective values are listed in Table 2.

As mentioned above, $\Delta\varepsilon$ does not depend on dc conductivity, unlike the chargeability $m$. Inasmuch as Eq. (3) for the chargeability includes $\sigma_0$, chargeability often correlates with the low-frequency dc resistivity $\rho = 1/\sigma_0$. Furthermore, at $c \cong 1$, the chargeability $m$ and the time constant $\tau$ are not independent (Kozhevnikov and Antonov, 2006).

The correlation between the Cole–Cole parameters is also manifested in the inversion results. In Fig. 7 the inversion results are plotted in the coordinates $\tau_1$ and $m_1$ (Fig. 7a), $\tau_1$ and $\Delta\varepsilon_1$ (Fig. 7b), $\rho_1$ and $m_1$ (Fig. 7c), and $\rho_1$ and $\Delta\varepsilon_1$ (Fig. 7d). The $m_1$ vs. $\tau_1$ plot in Fig. 7a demonstrates distinct correlation between the time constant and the chargeability, and there are no reasons to prefer any certain ($\tau_1$, $m_1$) point. As for the $\Delta\varepsilon_1$ vs. $\tau_1$ plot (Fig. 7b), the points here make up a compact "cloud". The small upward triangle marks the point the coordinates of which are $\tau_1$ and $\Delta\varepsilon_1$ averaged over all inversion data. Excluding from the inversion data set points 2 and 4 as "outliers" gives upon averaging the point shown as a downward triangle.

The inversion-derived $\rho_1$ and $m_1$ values exhibit a linear correlation (Fig. 7c), with a coefficient of determination $R^2 = 0.61$ in the case of all points included, or $R^2 = 0.83$ without point 3 (an outlier). As for the $\Delta\varepsilon_1$ vs. $\tau_1$ plot, here $R^2$ is 0.03 for all points and 0.16 with an outlier (point 4) excluded. These values of $R^2$ are very low indicating that, unlike $\rho_1$ and $m_1$, parameters $\rho_1$ and $\Delta\varepsilon_1$ are not correlated.

It is pertinent to comment briefly on the thickness $h_1$ and the resistivity $\rho_1$ of the upper layer. Their large scatter (Table 2) is due to S-equivalence rather than to random errors or low data quality: the variance of the conductance $S_1 = h_1/\rho_1$ (0.06 S on average) is quite small relative to the variances of $\rho_1$ and $h_1$ values.

Note that it was a polarizable layer overlying a non-polarizable basement that gave the best fit to the TEM data measured on the glacier. The ice being 500 m thick, one may wonder why the inversion resulted in "a layer" and not in a "half-space". In all probability, this is because a TEM response is specifically sensitive to the polarization induced in the upper layer of a thickness comparable with the transmitter loop size (Kozhevnikov and Antonov, 2009a, 2009b). Therefore, strictly speaking, the inversion results apply to the upper ~100 m of the glacier.

## 5. Discussion

In this section we discuss possible interpretations of the observed IP effects in terms of rock physics.

As reported in (Stognii, 2008; Stognii and Korotkov, 2010), the manifestations of inductive IP correlate spatially with areas where

**Table 2**
Results of single and joint inversion of coincident-loop TEM responses measured on a glacier. Loop sizes: 1 — 25 m × 25 m; 2 — 50 m × 50 m; 3 — 100 m × 100 m; 4 — 200 m × 200 m.

| 1 | 2 | 3 | 4 | $\rho_1$, Ω·m | $h_1$, m | $S_1$, S | $m_1$ | $\tau_1$, μs | $c_1$ | $\Delta\varepsilon_1$ | $\rho_2$, Ω·m | rms, % |
|---|---|---|---|---|---|---|---|---|---|---|---|---|
| + | | | | 400 | 21 | 0.053 | 0.19 | 17 | 0.79 | 1100 | 500 | 9.4 |
| | + | | | 47 | 3 | 0.060 | 0.086 | 18 | 0.97 | 4100 | 5000 | 8.6 |
| | | + | | 1360 | 130 | 0.10 | 0.56 | 34 | 0.69 | 660 | 560 | 33 |
| | | | + | 5000 | 370 | 0.074 | 0.7 | 93 | 0.74 | 4900 | 5000 | 33 |
| + | + | | | 950 | 60 | 0.065 | 0.15 | 21 | 0.99 | 440 | 4200 | 45 |
| + | + | + | | 5000 | 240 | 0.048 | 0.44 | 38 | 1 | 670 | 5000 | 70 |
| | + | + | | 780 | 30 | 0.038 | 0.28 | 26 | 0.9 | 1500 | 3500 | 56 |
| | | + | + | 3500 | 120 | 0.033 | 0.49 | 47 | 0.94 | 1500 | 4400 | 58 |
| Mean | | | | 2100 | 120 | 0.060 | 0.36 | 37 | 0.88 | 1900 | 3500 | 39 |
| Median | | | | 1200 | 90 | 0.056 | 0.36 | 30 | 0.92 | 1500 | 4300 | 39 |

+ symbol marks data used in inversion.

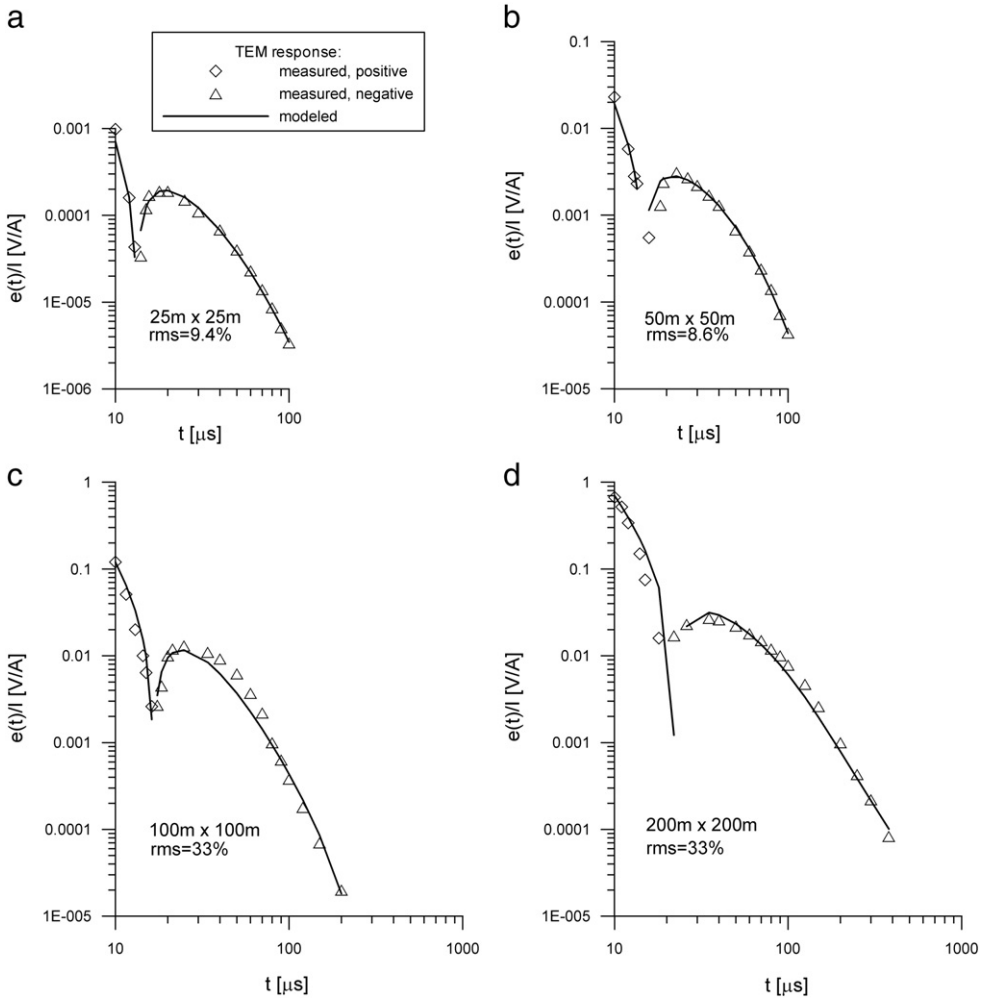


**Fig. 5.** Single inversion of TEM responses measured over a glacier.

near-surface geology is represented by sediments with high ice content. Thus it needs to be ascertained if ice which is an important constituent of frozen rocks may contribute to the fast-decaying IP, and if it does, to what extent. First we consider the dielectric relaxation in ice, as such, and then the Maxwell–Wagner (interfacial) polarization on the (ice inclusion)/(rock matrix) interface.

### 5.1. Dielectric relaxation in ice

As we wrote above, fast-decaying polarization in frozen ground fits the Debye relaxation model with $\tau \cong 100$ μs. According to the published evidence (Frolov, 1998; King and Smith, 1981), this combination of parameters ($c \cong 1$, $\tau \cong 100$ μs) is typical of freshwater polycrystalline ice. Therefore, the fast-decaying IP in permafrost might be associated with dielectric relaxation of ice in the pores.

The relative dielectric permittivity of water and ice is (Hippel, 1954; King and Smith, 1981)

$$\dot{\varepsilon} = \varepsilon_\infty + \frac{\varepsilon_s - \varepsilon_\infty}{1 + j\omega\tau}. \quad (11)$$

The relaxation of the orientational polarization of water molecules is fast ($\tau \cong 10^{-11}$ s), but the relaxation time becomes almost six orders of magnitude longer as water freezes to ice (Maeno, 1988; Purcell, 1986). For freshwater polycrystalline ice this time (in seconds) can be estimated as (King and Smith, 1981)

$$\lg\tau = 2900/T - 15.3\,, \quad (12)$$

where $T$ is the absolute temperature, °K. Thus calculated, $\tau \cong 20$ μs at subzero temperatures and increases to 20 ms when the temperature drops to −60° C. The ice permittivity $\varepsilon_s$ being of the order of 100 (Frolov, 1998; King and Smith, 1981) and $\varepsilon_\infty \cong 3$, one can assume that $\Delta\varepsilon \cong 10^2$.

In order to test the ice dielectric relaxation hypothesis, it is appropriate to estimate first the maximum possible effect. It is reasonable to imagine an ungrounded horizontal loop lay on an ice massif. With allowance made for the laboratory data, in this case (ice content 100 vol.%) inversion of the transient responses could be expected to give $\varepsilon_s - \varepsilon_\infty \cong 100$. Obviously, it is a maximum value of Δε that could be accounted for by the dielectric relaxation in ice with properties measured in laboratory. This value is more than three orders of magnitude lower than that found from inversion of TEM data (Table 1).

In the context of this study, it is pertinent to compare the TEM-derived polarization parameters ($\Delta\varepsilon$, $\tau$, $c$) for the Arctic glacier with those measured in laboratory. The inversion-derived exponent $c$ for massive ice (Table 2) approaches the unity, as in the case of the Debye relaxation observed in laboratory on monocrystalline ice samples and synthetic and natural polycrystalline ice (Frolov, 1998; Reynolds, 1985). Eq. (12) for ice at T = −10 °C gives $\tau \cong 50$ μs, which is similar to the $\tau$ values from laboratory dielectric measurements (Frolov, 1998; Maeno, 1988; Reynolds, 1985). Thus, the $\tau$ values listed in Table 2 approach those measured in laboratory and predicted by Eq. (12).

As for dielectric increment $\Delta\varepsilon$ ($\Delta\varepsilon \approx 10^3$) of in situ massive ice, it is at least ten times the laboratory measured values for freshwater polycrystalline ice ($\Delta\varepsilon \approx 10^2$). A reason of this difference remains open to speculation. As things now stands, we might think of this difference in a

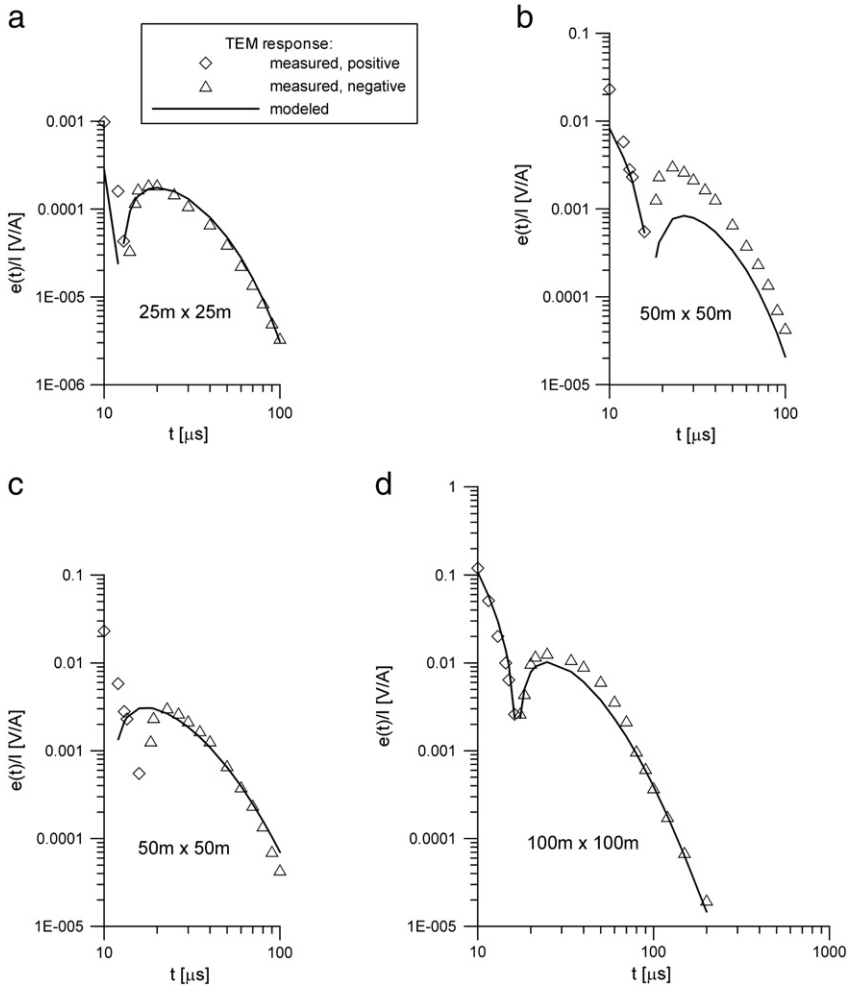


**Fig. 6.** Joint inversion of TEM responses measured over a glacier: (a, b) are for 25 m × 25 m (1) and 50 m × 50 m (2) loops, rms = 45%; (c, d) are for 50 m × 50 m (2) and 100 m × 100 m (3) loops, rms = 56%.

general sense as being manifestation of a "scaling". What is more important in the context of the problem under discussion is that $\Delta\varepsilon$ values measured over the glacier are tens to hundreds times lower than those obtained through inversion of TEM data from Yakutia ($1.5 \cdot 10^4$–$2 \cdot 10^5$). Thus, the TEM results from the glacier, and more so, the laboratory dielectric measurements on ice samples, show that the inductive IP effects observed in Yakutia hardly may result from dielectric relaxation intrinsic to ice.

### 5.2. Interfacial polarization

Frozen rocks are normally multiphase and heterogeneous, this being their inherent property resulting from their formation and changes. Heterogeneous systems, in turn, are known to exhibit dielectric dispersion at frequencies different from the respective frequencies of the system's individual components (Chelidze et al., 1977; Dukhin and Shilov, 1972). One of the mechanisms contributing to the frequency dependence of dielectric permittivity is the Maxwell–Wagner effect (Hippel, 1954): the electric field, applied to a material, charges each interface (even a microscopic one), the charge being proportional to the interface-orthogonal component of the macroscopic field and to the difference $(\varepsilon_1/\sigma_1) - (\varepsilon_2/\sigma_2)$ (Alvarez, 1973; Chelidze et al., 1977). Mathematically, this is an analog of polarization in dielectrics. The effect is often called "polarization by charge accumulation on the surfaces of inclusions" or *interfacial polarization*.

A large amount of experimental and theoretical work on the Maxwell–Wagner effect has been done as applied to synthetic heterogeneous materials (Chelidze et al., 1977; Dukhin and Shilov, 1972). The TEM survey people got interested in the problem in search for explanation of the monotony break in TEM responses measured in Yakutia. It was V. Sidorov (Molchanov and Sidorov, 1985; Sidorov, 1985, 1987) who drew attention to the problem and contributed a lot to its formulation. Although remaining within the limits of a flat capacitor model, he was the first to approach the low-frequency dielectric dispersion of frozen rocks in terms of interfacial polarization. He, together with his co-authors, undertook a pioneering study of the Maxwell–Wagner effect in borehole and in laboratory (Molchanov and Sidorov, 1985).

One can approximately estimate possible $\Delta\varepsilon$ due to the Maxwell–Wagner effect in frozen ground with a model of a porphyric rock (Artemenko and Kozhevnikov, 1999) which is simple enough not to require too many parameters and yields easily explainable results. Natural formations that fit this model include frozen rocks with simple (massive, basal, crust-like, or porphyry-like) cryostructures (Melnikov and Dubikov, 1986).

In calculations of dielectric permittivity, porphyric heterogeneous solids can be considered as two-phase mixtures comprising a continuous matrix of the dielectric permittivity $\varepsilon_1$ with embedded spherical inclusions of the permittivity $\varepsilon_2$. One of the best known formulas for the permittivity of a mixture belongs to Maxwell. The formula applies to mixtures with spherical inclusions the volumetric content $P$ of which is assumed to be relatively small (Hippel, 1954):

$$\varepsilon = \varepsilon_1 \left(1 + 3P \frac{\varepsilon_2 - \varepsilon_1}{\varepsilon_2 + 2\varepsilon_1}\right). \quad (13)$$

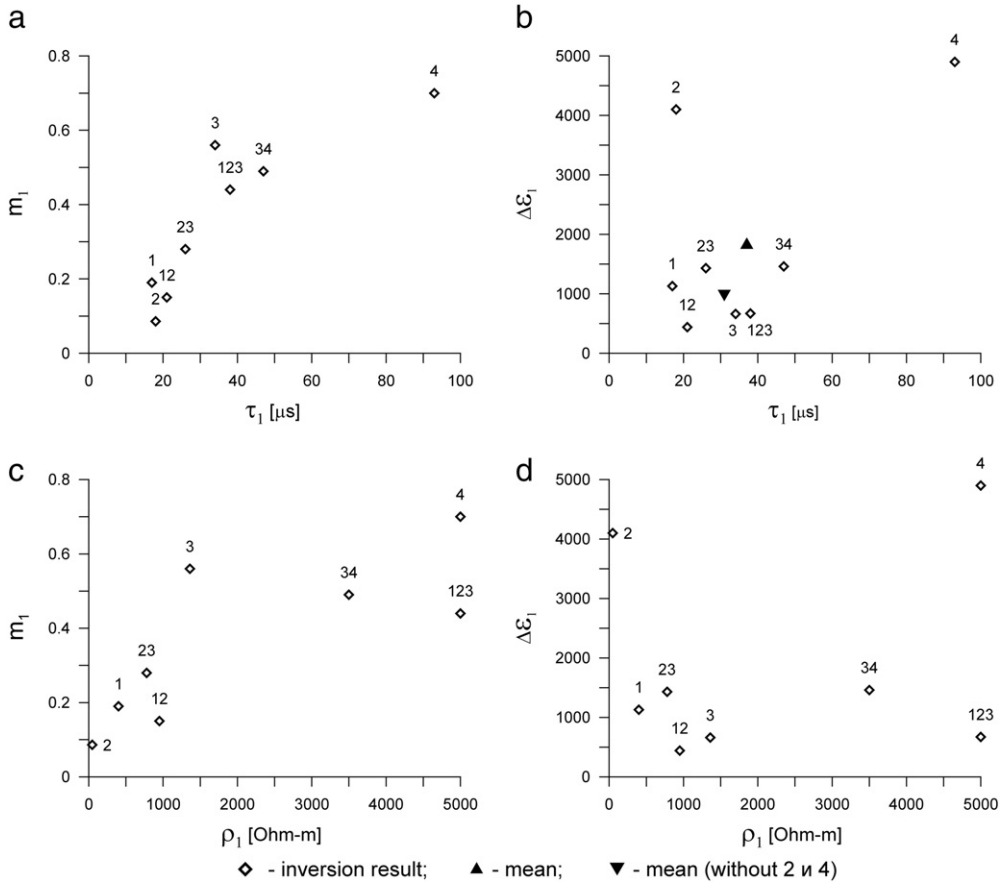


**Fig. 7.** Inversion results plotted in the coordinates: $\tau_1$ and $m_1$ (a), $\tau_1$ and $\Delta\varepsilon_1$ (b), $\rho_1$ and $m_1$ (c), $\rho_1$ and $\Delta\varepsilon_1$ (d).

Subject to the condition that the applied electric field is not vortex, Eq. (13) can be used to estimate the dielectric permittivity of a two-phase medium with regard to the Maxwell–Wagner effect (Chelidze et al., 1977; Dukhin and Shilov, 1972). Although being not true in the general case, this assumption may be a convenient approximation for low frequencies at which the electromagnetic wavelengths in any phase are much greater than the linear heterogeneity scale (in the case of TEM surveys, frozen rocks with heterogeneities existing as inclusions of interstitial ice, mineral grains, etc., obviously satisfy this condition). The advantage of this approximation is reducing the problem (mathematically) to the static case for ideal dielectrics.

Generally, the matrix and inclusions have complex permittivities ($\varepsilon_m^*$ and $\varepsilon_i^*$) and conductivities ($\sigma_m^*$ and $\sigma_i^*$). Then, for a porphyric rock, it is enough $\varepsilon_1^* = \varepsilon_m^* - j\frac{\sigma_m^*}{\omega\varepsilon_0}$ and $\varepsilon_2^* = \varepsilon_i^* - j\frac{\sigma_i^*}{\omega\varepsilon_0}$ to be substituted, respectively, for $\varepsilon_1$ and $\varepsilon_2$ in Eq. (13). Thus one arrives at Wagner's formula (Dukhin and Shilov, 1972):

$$\varepsilon^* = \varepsilon_1^*\left(1 + 3P\frac{\varepsilon_2^* - \varepsilon_1^*}{\varepsilon_2^* + 2\varepsilon_1^*}\right). \tag{14}$$

Thus found dielectric permittivity is complex and frequency-dependent even when the permittivity and conductivity of the matrix and of the inclusions do not depend on frequency. With the separated real and imaginary parts, Eq. (14) becomes

$$\varepsilon^* = \varepsilon' - j\varepsilon''. \tag{15}$$

Obviously, $\varepsilon'$has the meaning of the effective dielectric permittivity $\varepsilon_{\text{eff}}$ of a mixture while $\varepsilon''$ accounts for its effective conductivity $\sigma_{\text{eff}} = \omega\varepsilon_0\varepsilon''$:

$$\varepsilon^* = \varepsilon_{eff} - j\frac{\sigma_{eff}}{\omega\varepsilon_0}. \tag{16}$$

To estimate the order of magnitude of the Maxwell–Wagner polarization in frozen rocks, it is appropriate to use model of such a rock in which the mechanisms other than the Maxwell–Wagner polarization are as insignificant as possible. In this regard a good candidate is a frozen sand dielectric relaxation in which was studied extensively in laboratory (Frolov, 1998; Frolov and Fedyukin, 1983) and observed in the field (Kozhevnikov et al., 1995). Almost all interstitial water in sand, as well as in any coarse porous rock, turns into ice already at subzero temperatures. Only its small fraction (1–2% or less) remains unfrozen as inclusions and thin films. These films, coating mineral grains and ice inclusions, make up a quasi uniform matrix with the effective conductivity $\sigma_1$ of the order of $10^{-5}$–$10^{-3}$ S/m (Frolov, 1998; King et al., 1988). The conductivity of ice is much lower than that of the matrix. Because of this, such heterogeneous system can be presented as a relatively conducting continuous matrix with resistive ice inclusions (King et al., 1988).

Since the dielectric permittivity of bound water is much less than that of free water (Dukhin and Shilov, 1972) and its volumetric content is low in coarse-grained frozen rocks, the permittivity of the quasi-continuous matrix is mainly controlled by the permittivity of mineral grains. Thus, we assumed frozen sand to have $\varepsilon_1 \cong 5$. As for the ice inclusions, we assumed their dielectric permittivity $\varepsilon_2^*$ to be described by Debye formula (Eq. (11)), and the conductivity $\sigma_2$ was assumed to vary in the range $10^{-6}$–$10^{-4}$ S/m.

Fig. 8a illustrates the frequency dependence of the effective dielectric permittivity predicted by the wet frozen sand model consisting of a continuous matrix with $\varepsilon_1 = 5$, $\sigma_1 = 10 - 4$ S/m and inclusions with $\varepsilon_{2s} = 100$, $\varepsilon_{2\infty} = 3$, $\sigma_2 = 10^{-5}$ S/m. The dependences of $\varepsilon_{\text{eff}}$ on frequency $f$ are plotted for the relaxation times $\tau$ from 0 to 100 μs. According to Eq. (12), $\tau_2 = 30$ μs corresponds to the temperature of about −5 °C and 100 μs to −15 °C. The plots in Fig. 8*a* show that the effective time of dielectric relaxation of the frozen sand model

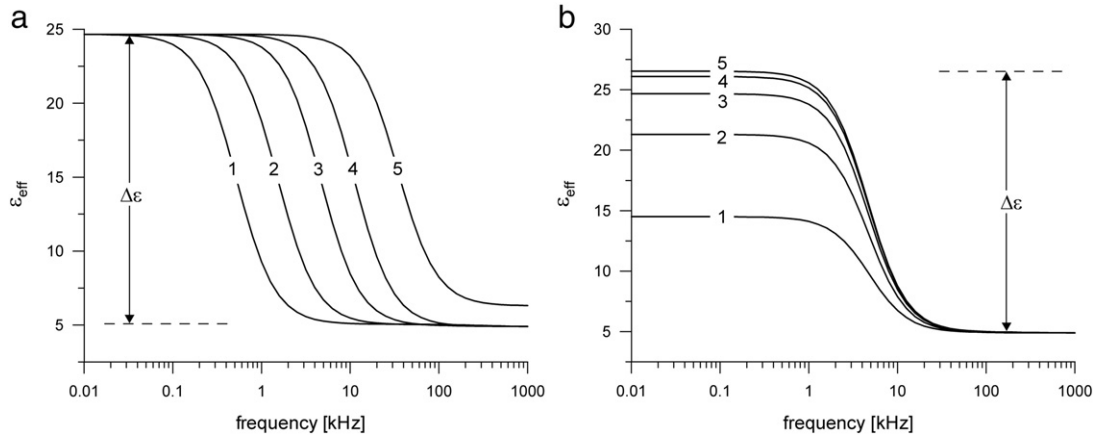


**Fig. 8.** Frequency dependencies of effective dielectric permittivity of a frozen sand with regard to Maxwell–Wagner effect at different $\tau_2$ (a): 1 — 300, 2 — 100, 3 — 30, 4 — 10, 5 — 0 μs; (other parameters: $\sigma_1 = 10^{-4}$ S/m; $\varepsilon_1 = 5$; $\sigma_2 = 10^{-5}$ S/m; $\varepsilon_{2s} = 100$; $\varepsilon_{2\infty} = 4$; $P = 0.1$) and the conductivity $\sigma_2$ of the inclusions (b): 1 — $10^{-4}$, 2 — $3 \cdot 10^{-5}$, 3 — $10^{-5}$, 4 — $3 \cdot 10^{-6}$, 5 — $10^{-6}$ S/m; (other parameters: $\sigma_1 = 10^{-4}$ S/m; $\varepsilon_1 = 5$; $\varepsilon_{2s} = 100$; $\varepsilon_{2\infty} = 4$; $\tau_2 = 30$ μs; $P = 0.1$).

increases proportionally to the Debye relaxation time of the ice inclusions.

Fig. 8b demonstrates how the ice conductivity influences the effective permittivity $\varepsilon_{eff}$ of the frozen sand model. As $\sigma_2$ decreases, the low-frequency values of $\varepsilon_{eff}$ increase; this increase is first rapid but then, after saturation at $\sigma_2 < 10^{-5}$ S/m, the low-frequency permittivity remains almost invariable. For the $\varepsilon_m(f)$ plots of Fig. 8b, the effective relaxation time of the model varies in the range 20–34 μs with relaxation time of inclusions held constant ($\tau_2 = 30$ μs).

The results shown in Fig. 8 indicate that taking into account the Maxwell–Wagner effect in the case of a porphyric frozen rock predicts dielectric relaxation at frequencies that fall into the spectrum typical of the TEM signals. However, the dielectric increment $\Delta\varepsilon \cong \varepsilon_s$, an *amplitude* parameter, is four orders of magnitude lower than that found through inversion of TEM data (Table 1).

It should be noted that the plots of Fig. 8 were calculated for volumetric ice content $P = 0.1$, though on occasion it may reach 50% or more in the near-surface frozen ground of Western Yakutia (Klimovsky and Gotovtsev, 1994). In such an event the Maxwell's formula may result in underestimating the permittivity response, and the Bruggeman–Hanai equation for the complex dielectric permittivity of a concentrated suspension would give more correct estimates of $\Delta\varepsilon$ (Chelidze and Gueguen, 1999; Hanai, 1968). However, these errors are of no importance in the context of our study since the case in point is not the exact calculation of Δε but estimating the order of its magnitude. We used the Maxwell formula because, unlike the Hanai equaition, it enables straightforward calculation of the complex permittivity response. In any case, even if we assume $\Delta\varepsilon \cong 1000$, this value is more than hundred times as low as those listed in Table 1.

In Artemenko and Kozhevnikov (1999), the dielectric permittivity calculated with Eq. (14) is compared with laboratory data for frozen rocks (Frolov, 1998). Frozen sand has $\Delta\varepsilon$ several times that found with Eq. (14) at subzero temperatures but the measured and calculated data agree well at −15 °C. Yet, neither the misfit (at about 0 °C) nor the fit (at −15 °C) between the measured and calculated values is of importance in estimating the order of the effects: the $\Delta\varepsilon$ values measured on frozen sand samples are within a few hundreds (at ~40 vol.% water). Therefore, laboratory values of the dielectric increment as well are at least thousand times different from those found through inversion of TEM data (Table 1).

Thus, dielectric relaxation of ice and/or the Maxwell–Wagner polarization cannot account for the high Δε values predicted by the TEM data inversion. That is why we still have to address the question of what phenomenon may account for the frequency dependence of conductivity and/or dielectric permittivity of frozen ground and primarily for very large $\Delta\varepsilon$ values. An overview of recent publications on IP manifestations in unconsolidated wet rocks suggests the electrochemical polarization formulated in terms of a surface conduction as a likely candidate.

### 5.3. Surface conduction

The surface contribution to processes associated with electrochemical polarization is known to have several controls (Chelidze and Gueguen, 1999; Chelidze et al., 1999): (1) the surface-to-volume ratio (specific surface area) of the components; (2) the surface and volume physical and chemical properties of the components; (3) the mode of coupling between surface and volume processes; (4) the characteristics of the electrical double layer (EDL) at the solid–liquid interface; (5) the geometrical, chemical, or electrical heterogeneity of the interfaces.

Obviously a water-bearing frozen rock can polarize under a great variety of the above controls. Taking them all into account in a polarization model of frozen ground, with all their interactions, is obviously a challenge not to meet in the nearest future.

In this respect, an alternative model may be of interest in which the complex conductivity of a rock is a sum of bulk and surface conductivities (Lesmes and Friedman, 2005; Lesmes and Frye, 2001; Slater and Lesmes, 2002; Vinegar and Waxman, 1984; Lesmes, 2001; Slater and Glaser, 2003; Slater et al., 2006), which corresponds to the case of parallel conduction paths. The effective conductivity of a small rock volume or sample shown as a parallel equivalent circuit in Fig. 9a is

$$\sigma^*(\omega) = (\sigma_{bulk} + j\omega\varepsilon_0\varepsilon_\infty) + \left[\sigma'_{surf}(\omega) + j\sigma''_{surf}(\omega)\right], \quad (17)$$

where $\sigma_{bulk}$ and $\varepsilon_\infty$ are the bulk (low-frequency) conductivity and the high-frequency dielectric permittivity of the rock sample, and $\sigma'_{surf}(\omega)$ and $\sigma''_{surf}(\omega)$ are the real and imaginary surface conductivity components. Combining the real and imaginary components in Eq. (17) gives

$$\sigma^*(\omega) = \left[\sigma_{bulk} + \sigma'_{surf}(\omega)\right] + j\left[\omega\varepsilon_0\varepsilon_\infty + \sigma''_{surf}(\omega)\right]. \quad (18)$$

Since $\omega\varepsilon_\infty\varepsilon_0 << \sigma''_{surf}(\omega)$, at low frequencies where IP processes are commonly measured in the field, the effective conductivity is

$$\sigma^*(\omega) = \left[\sigma_{bulk} + \sigma'_{surf}(\omega)\right] + j\sigma''_{surf}(\omega). \quad (19)$$

The imaginary component of conductivity, within the limits of the discussed model and within the frequency range common to the TEM signals spectra, is controlled by the surface conductivity. As for the real conductivity component, it includes the contributions from

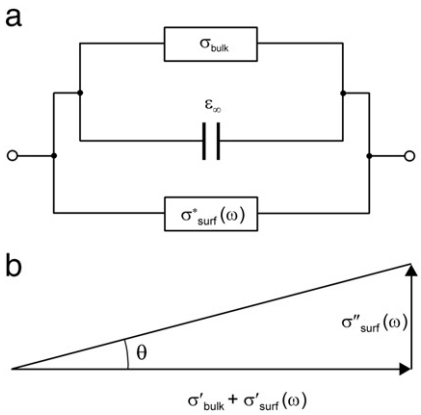


**Fig. 9.** (a) Parallel equivalent circuit presentation of a rock conductance (Lesmes and Frye, 2001; Vinegar and Waxman, 1984). The bulk conductivity $\sigma_{bulk}$ of electrolyte in pores does not depend on frequency and causes no capacitance effects. The high-frequency dielectric permittivity $\varepsilon_\infty$ defines the high-frequency capacitance of the system. The IP effects are attributed to the imaginary component $\sigma''_{surf}(\omega)$ of the surface conductivity. (b) Relationship of the phase angle $\theta$ with the real and imaginary components of the complex conductivity.

both bulk and surface conductivities. The vector diagram in Fig. 9b shows the relationship between the real and imaginary conductivity components and the phase shift ($\theta$).

The bulk rock conductivity $\sigma_{bulk}$ is independent of frequency and is given by the Bruggeman–Hanai–Sen (BHS) equation (Lesmes, 2005)

$$\sigma_{bulk} = \sigma_w \phi^n, \tag{20}$$

where $\sigma_w$ is the conductivity of the pore solution (interstitial water), $\phi$ is the porosity, and $n$ is the cementation index which is a function of the effective grain shape. This relationship was first derived empirically by Archie (1942).

Electrochemical polarization at the solid–fluid interface causes the frequency dependence of the complex conductivity $\sigma^*_{surf}(\omega)$. When $\omega \to 0$, the imaginary component of the surface conductivity tends to zero while the in-phase component tends to the constant $\sigma'_{surf}(0)$. The dc component of the surface conductivity is given by Lesmes and Frye (2001).

$$\sigma'_{surf}(0) = \lim_{\omega \to 0} \sigma'_{surf}(\omega) = \frac{e\mu_s \Sigma_0 S_0}{f_g}, \tag{21}$$

where $e$ is the electron charge, $\mu_s$ is the effective surface ionic mobility, $\Sigma_0$ is the mineral surface charge density, $S_0$ is the weighted surface-to-volume ratio, $f_g$ is a geometric factor that characterizes the tortuosity of the grain/pore interface.

According to Lesmes and Frye (2001), the complex surface conductivity response at an arbitrary frequency can be written as a product of the dc surface conductivity and a spectral response function $J^*(\omega, g(r), \mu_s)$:

$$\sigma^*_{surf}(\omega) = \frac{e\mu_s \Sigma_0 S_0}{f_g} J^*[\omega, g(r), \mu_s], \tag{22}$$

where $J^*(\omega, g(r), \mu_s)$ is obtained by convolving the electrochemical polarization response of the fixed and diffuse EDL parts for a single grain/pore surface with the radius $r$ and the distribution $g(r)$ of the grain/pore sizes. The magnitude of the complex conductivity response is defined primarily by the product of $S_0$, $\Sigma_0$, and $\mu_s$, while its frequency dependence is a function of the grain/pore size distribution (Lesmes and Frye, 2001).

Fig. 10 is a sketched version of Fig. 6 from Lesmes and Frye (2001), representing complex responses of water-saturated Berea sandstone. These data illustrate the main features of complex conductivity frequency response observed on wet porous rocks. The (a) and (b) panels of the figure give, respectively, the plots of $\sigma' = \sigma_{bulk} + \sigma'_{surf}$ and $\sigma'' = \sigma''_{surf}$. Panel (c) shows the real dielectric permittivity $\varepsilon'$ related with the imaginary conductivity as (Lesmes and Friedman, 2005)

$$\varepsilon' = \frac{\sigma''}{\omega \varepsilon_0}. \tag{23}$$

At very low frequencies (0.01 Hz and less), $\sigma''$ tends to zero when $\omega \to 0$, while $\varepsilon'$ remains almost invariable approaching asymptotically the low-frequency limit $\varepsilon'_s$. Above 0.1 MHz $\varepsilon'$ tends to the high-frequency limit ($\varepsilon'_\infty$) and $\sigma''$ increases proportionally to frequency.

The increment of real permittivity for the frequency range typical of the TEM signals spectra (Fig. 10c) is of the same order of magnitude as $\Delta\varepsilon$ values inferred from TEM data (Table 1). Thus, the surface conductance model may account for the giant low frequency dielectric permittivities recovered from the inversion of TEM data.

Since porous sedimentary rocks are of broad occurrence everywhere, it reasonably to ask a question why it is Yakutia where from the IP effects are so largely reported to manifest during TEM surveys? A plausible explanation may be that depending on whether the same rock is frozen or not the contributions of surface and bulk conductivities to a total response are very different.

Fig. 11a shows a rock volume with mineral grains and pore fluid. At positive temperatures, the conductive fluid fills the whole pore space, and the bulk conductivity predominates over the surface one ($\sigma'' \ll \sigma'$). In this case the chargeability being proportional to $\tan^{-1}(\sigma''/\sigma') \cong \sigma''/\sigma'$ (Slater and Lesmes, 2002) is low, and the IP effects are weak, correspondingly. At temperatures below zero, the pore water freezes and only its minor portion remains unfrozen in the adsorbed form as thin films on grain/iced pore interfaces (Fig. 11b).

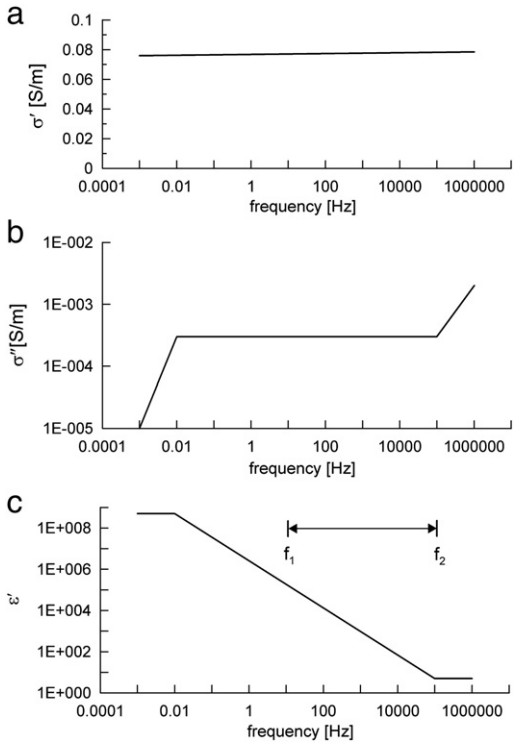


**Fig. 10.** The real (a) and imaginary (b) components of conductivity, and the real component of dielectric permittivity (c) of water-saturated Berea sandstone as a function of frequency: a sketched version of Fig. 6 from Lesmes and Frye (2001). Horizontal line with arrows in (c) shows the frequency bandwidth ($f_1 \cong 10$ Hz, $f_2 \cong 10^5$ Hz) typical of the TEM signals spectra.

Thereby the bulk conductivity strongly decreases and the rock conductivity becomes tens or hundreds times lower (Frolov, 1998; King et al., 1988). Unlike the bulk conductivity, the surface conductivity depends on the surface-to-volume ratio of the pores which does not decrease as the rock freezes up. Moreover, inasmuch as the processes at the ice–water interface are the same as at the mineral–water interface (Deryagin et al., 1989; Nechaev and Ivanov, 1974), it is reasonable to expect that interstitial water freezing would increase the surface-to-volume ratio at about twice (Fig. 11b). Finally, one more cause of a greater surface conductivity contribution to the response might be that freezing pore water increases the salinity of the small portion of remaining unfrozen fluid (Frolov, 1998; King et al., 1988).

On the other hand, there is no plausible explanation, in terms of the electrochemical polarization, for the time constants recovered from the TEM data. In modern literature the electrochemical polarization is attributed (1) to the polarization of the Stern layer of the electrical double layer surrounding grain particles or/and (2) to the membrane polarization. In such a case the relaxation time $\tau$ is directly proportional to the square of the grain radius $a$ (or of the pore throat size), and inversely proportional to the ion diffusivity $D$ (Santamarina et al., 2001),

$$\tau = \frac{a^2}{2D}. \tag{24}$$

Using the average value of $\tau$ recovered through inversion of the TEM data (100 μs) and the standard value of $D$ for ions in water solution ($\sim 10^{-9}$ m$^2$ s$^{-1}$) one can obtain the grain radius of about $5 \cdot 10^{-7}$ m. This means that the polarization is related to clay particles only. Moreover assuming the surface diffusion at play ($D < 10^{-10}$ m$^2$ s$^{-1}$) one obtains the grain radius of about $1.5 \cdot 10^{-7}$ m and less.

The mere conclusion that fast-decaying polarization of the near-surface frozen rocks in Western Yakutia might be due to the presence of clay particles should present no problem. Unconsolidated sediments in this region are known to be rather heterogeneous and to contain in abundance a loamy material (Alekseev, 2009; Klimovsky and Gotovtsev, 1994). Furthermore, some Paleozoic rocks originally contain clay particles that form interbeds (clayey limestone and dolomite) or cement (marl, siltstone, mudstone) (Kobranova, 1986).

More importantly is that in typical cases of the electrochemical polarization of clayey and clay free rocks the relaxation time distribution is large (Bittelli et al., 2004; Frolov, 1998; Lesmes and Frye, 2001). Electrochemical polarization usually does not fit single Cole–Cole model, and multi-Cole–Cole approximation is frequently used. Also in these approximations typically the exponent $c$ is much smaller than 1. Thus, the values of the Cole–Cole exponent $c$ recovered through inversion of the TEM data seem to be inconsistent with known results of research into electrochemical polarization of wet porous rocks.

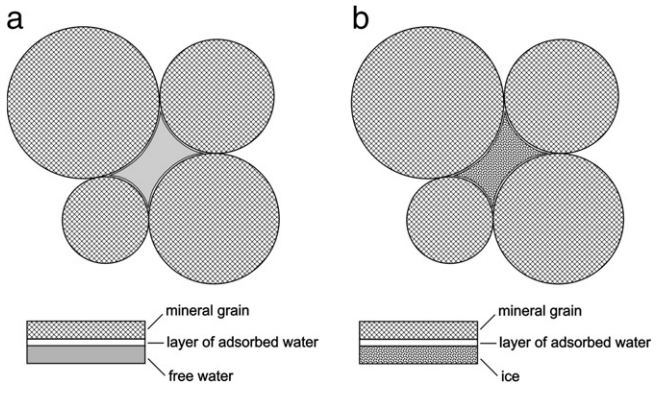


**Fig. 11.** A volume of a water-saturated rock at temperatures above (a) and below (b) 0 °C.

This brings up the question on the resolution of the Cole–Cole exponent. Usually, it is not well resolved in IP inversions, which does not constitute a problem because it is not extensively used. However, in this paper, it plays an important role, and therefore it is essential to understand how well it can actually be determined. It is appropriate at this point to refer to a resent paper by Kozhevnikov and Antonov (2008) where by means of numerical simulation experiment with homogeneous polarizable half-space was demonstrated that $c$ values recovered from inversion of IP-affected TEM data differed from true ones by no more than ±20% in the case of small $c$ and/or $m$ ($c < 0.2$, $m < 0.02$). For models with their parameters within the range constrained by $c > 0.2$ and $m > 0.02$, the error in $c$ inversion did not exceed a few percent.

Related numerical experiment was applied to explore the potentialities and the limitations of the inversion of IP-affected TEM responses of a two-layer earth (Kozhevnikov and Antonov, 2010). Two sets of models were used in these studies: (1) with a polarizable layer overlying a non-polarizable basement, and (2) with a non-polarizable layer overlying a polarizable basement. Inversion of TEM responses for models of set 1 resulted in an excellent recovery of the Cole–Cole parameters, exponent $c$ included. For the models from set 2 the Cole–Cole parameters were close to the true ones if the thickness of the upper layer was small. Increasing the thickness of the upper layer resulted in problems in recognizing whether the layer or basement was polarizable and in large errors in the Cole–Cole parameters. It is important in the context of this paper that when large errors occurred in determining $c$, it was always *underestimated*.

The above considerations suggest that the Cole–Cole exponent recovered through inversion of the TEM data is well resolved. This leads one to consider the values of $c$ from Western Yakutiya as reliable ones.

As things now stand, a satisfactory explanation of the above inconsistencies remains open to speculations. Nevertheless, it may be useful to discuss some plausible reasons why inversion of the TEM responses resulted in the Cole–Cole model with small $\tau$ and $c \cong 1$.

First, it should be noted that, when speaking about inductive IP, one usually implies the polarization processes that are fast as compared to those measured with conventional IP technique. In studies of slow IP processes inductive measurement systems are less efficient as those using galvanic contact with the ground. Because on a time scale characteristic of slow IP phenomena the primary vortex electric field produced by current switch-off in a transmitter loop has a small duration, the polarization stops well before it reaches its maximum. On the other hand, since after current turn-off in a transmitter loop the polarization currents and their (secondary) magnetic field decays slowly, according to Faraday's law, only small voltage is induced in a receiver loop. As a consequence inductive IP method is sensitive predominately to a fast-decaying component of a total IP response.

In this regard we have to mention a resent publication by Ageev (2011), who measured time-domain IP responses of frozen sand and clay in the time range 20 μs–1 s. The measurements were made in field and on both core and artificial samples using four-electrode systems. In all cases a total IP response represented a sum of fast- and slowly-decaying processes. Thus fitting the field data with the Cole–Cole model resulted in $\tau = 80$μs and $c = 0.82$ for the fast-decaying polarization, whereas in $\tau = 10$ ms and $c = 0.32$ for the slowly-decaying one. It was shown during laboratory experiments that the fast-decaying process arosed only upon freezing a sample. On further lowering the temperature from −1 °C to −20 °C, the magnitude of the fast-decaying process (in terms of chargeability, $m$) increased whereas that of slowly-decaying one decreased.

There is another reason why inductively induced polarization may appear mostly in the presence of frozen rocks. Being formulated in a simplified way, it is as follows. TEM responses of a polarizable ground result from competition between the IP and “normal” (decaying eddy

currents), transient processes (Fig. 1). Other things being equal, the relation of the induction and polarization processes depends on the conductivity of rocks: the lower the conductivity the greater is the relative contribution of the IP process to the total response (Kozhevnikov and Antonov, 2009a). As a wet rock freezes up, it becomes at least one order of magnitude more resistive, and the IP contribution increases relative to the EM effects. Thus, the IP effects are inconspicuous against the induction ones while interstitial water remains unfrozen, but upon freezing of the pore water $\sigma'$ becomes low, the eddy currents decay rapidly, and the total response is due predominately to the IP effects.

Note that a frozen rock is in some respects similar to a dry one with air in its pores (Frolov, 1998). As in the case of frozen rocks the conductance of dry porous materials is due to thin films of bound water. Therefore, one may expect IP effects to manifest in TEM responses measured over dry porous rocks, as in the case of TEM survey carried out in and around the caldera of the Fogo volcano (Descloitres et al., 2000). Inversion of TEM data, measured in the resistive environment of the Fogo volcano, indicated a fast-decaying IP with $m = 0.8$, $\tau = 20$ μs, and $c = 0.8$. It is interesting that these Cole–Cole parameters are close to those reported from the cold regions (Table 1).

## 6. Conclusions

TEM data from Yakutia and other northern areas of widespread permafrost are affected by the fast decaying polarization of wet frozen rocks. The inversion of TEM data from Yakutia in terms of the Cole–Cole model gave the chargeability $m$ in the range 0.2 to 0.85, mostly within 0.2–0.5, and the relaxation time constant from 35 to 250 μs (50 to 100 μs on average), but a much less variable exponent $c$ (0.8 to 1). The fact that most often $c$ is close to unity is evidence of a narrow range of relaxation times (Debye-type process). Therefore, one can convert the chargeability, using Eq. (9), into low-frequency relative dielectric permittivity that was found to be tens to a few hundreds of thousands. The proximity of the Cole–Cole exponent to unity suggested that the fast-decaying polarization in permafrost might be due to dielectric relaxation of ice inclusions and/or to the interfacial polarization. Both models predict a Debye dielectric relaxation in frozen rocks at frequencies characteristic of the TEM signals spectra, but the dielectric increment (actually low-frequency permittivity) implied by those models is three or four orders of magnitude lower than the values recovered through the inversion of the Yakutia TEM data.

Inversion of TEM responses measured on an Arctic glacier gave the dielectric relaxation time$\tau$ and the exponent $c$ close to those measured in laboratory on samples of synthetic and natural ice and those typical of permafrost in Yakutia, but the dielectric increment turned out to be 2–3 orders of magnitude lower ($1.5 \cdot 10^4$–$2 \cdot 10^5$ against $\approx 10^3$) than that of frozen Yakutia rocks.

A most likely reason of the high low-frequency dielectric permittivity is electrochemical polarization of the films of unfrozen water that stays, upon rock freezing, adsorbed on the surfaces of mineral grains and ice inclusions.

It is convenient to describe and simulate the electrochemical polarization effects in terms of frequency-dependent surface conductivity related with the surface-to-volume ratio, which, in turn, depends on dispersivity of rocks.

There are two reasons why IP effects may appear over permafrost so often. One explanation, in terms of rock physics, is that both real and imaginary components of the surface conductivity remain inconspicuous against the bulk one while pore fluid is unfrozen. However, upon freezing the interstitial water, the bulk conductivity tends to zero while the surface conductivity, its imaginary component included, remains invariable. This enhancement of the imaginary conductance contribution into the total response manifests as an increase in the chargeability. The other reason is EM by its nature: the relative contribution of the eddy currents becomes less than that of IP as a result of the conductivity drop associated with freezing.

The fact that wet frozen rocks show a narrow distribution of IP relaxation times remains open to speculation. It may indicate the incompleteness of the available theoretical and experimental models and the necessity for further laboratory and especially field measurements of low-frequency dielectric properties of frozen rocks.

## Acknowledgments

The authors thank A. Hördt and an anonymous reviewer for their helpful comments and suggestions, which greatly improved both the general structure and the style of the paper.

## References

Ageev, V.V., 2011. Laboratory-scale induced polarization measurements on frozen rock samples. Proc. V All-Russian M.N. Berdichevsky and L.L. Vanyan Workshop on Electromagnetic Sounding of the Earth: EMS-2011, St. Petersburg, 16–21 Mai 2011, Vol. 2. St. Petersburg University, pp. 11–14.
Alekseev, S.V., 2009. Cryological–Hydrogeological Systems of the Yakutia Diamond Province. [in Russian] GEO, Novosibirsk.
Alvarez, R., 1973. Complex dielectric permittivity in rocks: a method for its measurement and analysis. Geophysics 38 (5), 920–940.
Antonov, E. Yu, Kozhevnikov, N.O., Korsakov, M.A., 2010. The TEM-IP program for inversion of IP-affected TEM data. Proc. 1st International R&D Conf. GEOBAIKAL-2010 on EM Methods. Irkutsk. 2 pp.
Archie, G.E., 1942. The electrical resistivity log as an aid in determining some reservoir characteristics. Transactions of the American Institute of Mining, Metallurgical and Petroleum Engineers 146, 54–62.
Artemenko, I.V., Kozhevnikov, N.O., 1999. Modeling the Maxwell–Wagner effect in coarse unconsolidated frozen ground [in Russian] Kriosfera Zemli III (1), 60–68.
Bittelli, M., Flury, M., Roth, K., 2004. Use of dielectric spectroscopy to estimate ice content in frozen porous media. Water Resources Research 40 (W04212), 1–11. doi:10.1029/2003WR002343.
Chelidze, T.L., Gueguen, Y., 1999. Electrical spectroscopy of porous rocks: a review — 1. Theoretical models. Geophysical Journal International 137, 1–15.
Chelidze, T.L., Derevyanko, A.I., Kurilenko, O.D., 1977. Electric Spectroscopy of Heterogeneous Systems. [in Russian] Naukova Dumka, Kiev.
Chelidze, T.L., Gueguen, Y., Ruffet, R., 1999. Electrical spectroscopy of porous rocks: a review — 2. Experimental results and interpretation. Geophysical Journal International 137, 16–34.
Deryagin, B.V., Kiseleva, O.A., Sobolev, V.D., 1989. Flow of nonfreezing water in porous solids. In: Deryagin, B.V., Churaev, N.V., Ovcharenko, F.D. (Eds.), Water in Disperse Systems. Khimiya, Moscow, pp. 101–115. [in Russian].
Descloitres, M., Guerin, R., Albouy, Y., Tabbagh, A., Ritz, M., 2000. Improvement in TDEM sounding interpretation in presence of induced polarization. A case study in resistive rocks of the Fogo volcano, Cape Verde Islands. Journal of Applied Geophysics 45, 1–18.
Dukhin, S.S., Shilov, V.N., 1972. Dielectric Phenomena and the Double Layer in Disperse Systems and Polyelectrolytes. Naukova Dumka, Kiev. [in Russian].
Flis, F.M., Newman, G.A., Hohman, G.W., 1989. Induced-polarization effects in time-domain electromagnetic measurements. Geophysics 54, 514–523.
Frolov, A.D., 1998. Electrical and Elastic Properties of Ice and Frozen Rocks. [in Russian] ONTI PC RAN, Pushchino.
Frolov, A.D., Fedyukin, I.V., 1983. Polarization of frozen disperse rocks in alternating electric fields. Izvestiya Vuzov, Geologiya i Razvedka 6, 90–96.
Hanai, T., 1968. Electrical properties of emulsions. In: Sherman, P. (Ed.), Emulsion Science. Academic Press, New York, pp. 354–478.
Hippel, A.R., 1954. Dielectrics and Waves. John Wiley, New York.
King, R.W.P., Smith, G.S., 1981. Antennas in matter: fundamentals. Theory and Applications. MIT Press, MA.
King, M.S., Zimmerman, R.W., Corwin, R.F., 1988. Seismic and electrical properties of unconsolidated permafrost. Geophysical Prospecting 36, 349–364.
Klimovsky, I.V., Gotovtsev, S.P., 1994. The Kryolithosphere of the Yakutian Diamond Province. [in Russian] Nauka, Novosibirsk.
Kobranova, V.N., 1986. Petrophysics. A University Course. [in Russian] Nedra, Moscow.
Kozhevnikov, N.O., Antonov, E.Y., 2006. Fast-decaying IP in frozen unconsolidated rocks and potentialities for its use in permafrost-related TEM studies. Geophysical Prospecting 54, 383–397.
Kozhevnikov, N.O., Antonov, E.Yu., 2008. Inversion of TEM data affected by fast-decaying induced polarization: numerical simulation experiment with homogeneous half-space. Journal of Applied Geophysics 66, 31–43.
Kozhevnikov, N.O., Antonov, E.Yu., 2009a. TEM soundings of polarizable earth. Geofizicheskii Zhurnal 31 (4), 104–118.
Kozhevnikov, N.O., Antonov, E.Yu., 2009b. Joint inversion of IP-affected TEM data. Russian Geology and Geophysics 50 (2), 136–142.
Kozhevnikov, N.O., Antonov, E.Yu., 2010. Inversion of IP-affected transient responses of a two-layer earth. Russian Geology and Geophysics 51 (6), 708–720.
Kozhevnikov, N.O., Artemenko, I.V., 2004. Modeling the effect of dielectric relaxation in frozen ground on TEM responses. Kriosfera Zemli VIII (2), 30–39.

Kozhevnikov, N.O., Nikiforov, S.P., Snopkov, S.V., 1995. Field studies of fast-decaying IP processes in frozen ground. Geoekologiya 2, 118–126.
Krylov, S.S., Bobrov, N.Yu., 1998. Anomalous electrical properties of saline permafrost on the Yamal Peninsula, North-Western Siberia, from field electromagnetic survey. PERMAFROST — Seventh International Conference (Proceedings), Yellowknife (Canada): Collection Nordicana, 55, pp. 611–616.
Krylov, S.S., Bobrov, N.Yu., 2002. Frequency dispersion of electrical properties of frozen ground: TEM sounding application. Kriosfera Zemli VI (3), 59–68.
Lee, T., 1981. Transient response of a polarizable ground. Geophysics 46, 1037–1041.
Lesmes, D.P., 2001. Dielectric spectroscopy of sedimentary rocks. Journal of Geophysical Research 106 (B7), 13, 329–13, 346.
Lesmes, D.P., Friedman, Sh.P., 2005. Relationships between the electrical and hydrogeological properties of rocks and soils. In: Rubin, Y., Hubbart, S.S. (Eds.), Hydrogeohysiscs. Springer, pp. 87–128.
Lesmes, D.P., Frye, K.M., 2001. Influence of pore fluid chemistry on the complex conductivity and induced polarization response of Berea sandstone. Journal of Geophysical Research 106 (B3), 4079–4090.
Maeno, N., 1988. The Ice Science. [Russian Translation from Japanese] Mir, Moscow.
Melnikov, E.S., Dubikov, G.I. (Eds.), 1986. Methods of Regional Engineering Cryological Studies for Plainland Terrains. Nedra (VSEGINGEO), Moscow. [in Russian].
Problems of Polarization of Rocks. [in Russian] In: Molchanov, A.A., Sidorov, V.A. (Eds.), VINITI Reports, N 5847-85. 109 pp.
Nechaev, E.A., Ivanov, I.A., 1974. The electric double layer at the ice–solution interface. Kolloidnyi Zhurnal XXXVI, 583–584 (3, May–June).
Ogilvi, A.A., 1990. Fundamentals of Engineering Geophysics. A University Course. [in Russian] Nedra, Moscow.
Olenchenko, V.V., Kozhevnikov, N.O., Matrosov, V.A., 2008. Fast-decaying induced polarization of the near-surface frozen rocks of the Mirny kimberlite field. 3rd Saint Petersburg International Conference & Exhibition, 7–10 April 2008, Lenexpo, Saint Petersburg, Russia, p. C010 (6 pp.).
Olhoeft, G.R., 1978. Electrical properties of permafrost. Proceedings Third International Conference on Permafrost, Vol. 1. National Research Council of Canada, Ottava, pp. 127–131.
Pelton, W.H., Ward, S.H., Hallof, P.G., Sill, W.R., Nelson, P.H., 1978. Mineral discrimination and removal of inductive coupling with multifrequency IP. Geophysics 43, 588–609.
Purcell, E.M., 1986. Electricity and magnetism, 2nd edition. Berkeley Physics Course, vol. II. McGraw Hill. Education.
Reynolds, J.M., 1985. Dielectric behaviour of firn and ice from the Antarctic peninsula, Antarctica. Journal of Glaciology 31 (109), 253–262.
Santamarina, J.C., Klein, K.A., Fam, M.A., 2001. Soil and Waves. John Wiley& Sons, Inc., New York.
Sidorov, V.A., 1985. The TEM sounding method. [in Russian] Nedra, Moscow.
Sidorov, V.A., 1987. On electrical chargeability of nuniform rocks. Izvestiya Akademii Nauk SSSR, Fizika Zemli 10, 58–64.
Slater, L.D., Glaser, D.R., 2003. Controls on induced polarization in sandy unconsolidated sediments and application to aquifer characterization. Geophysics 68, 1547–1558.
Slater, L., Lesmes, D., 2002. IP interpretation in environmental investigations. Geophysics 67, 77–88.
Slater, L., Ntarlagiannis, D., DeBonne, W., 2006. On the relationship between induced polarization and surface area in metal–sand and clay–sand mixtures. Geophysics 71 (2), A1–A5. doi:10.1190/1.2187707.
Smith, R.S., Klein, J., 1996. A special circumstance of airborne induced-polarization measurements. Geophysics 61, 66–73.
Smith, R.S., Walker, P.W., Polzer, B.D., West, G.F., 1988. The time-domain electromagnetic response of polarizable bodies: an approximate convolution algorithm. Geophysical Prospecting 36, 772–785.
Stognii, V.V., 2008. TEM surveys of polarizable frozen ground in the Yakutia kimberlite province. Kriosfera Zemli XII (4), 46–56.
Stognii, V.V., Korotkov, Yu V., 2010. TEM Surveys for Kimberlite Exploration. [in Russian] Malotirazhnaya Tipografiya 2D, Novosibirsk. 121 pp.
Vanchugov, V.A., Kozhevnikov, N.O., 1998. Investigating the geoelectrical structure of the Nakyn kimberlite field in Western Yakutiya with the TEM method. [in Russian] In: Uchitel, M.S. (Ed.), Geology, Prospecting and Exploration of Mineral Deposits. Collection of Papers. : Transactions of Irkutsk Technical University,Issue 22. Irkutsk Technchal University, Irkutsk, pp. 164–176.
Vinegar, H.J., Waxman, M.H., 1984. Induced polarization of shaly sands. Geophysics 49, 1267–1287.
Vostretsov, R.N., Molchanov, A.A., Sidorov, V.V., 1985. TEM processes in massive ice. In: Molchanov, A.A., Sidorov, V.A. (Eds.), Problems of Polarization of Rocks. VINITI Reports, N 5847-85, pp. 58–64. [in Russian].
Wait, J.R., 1982. Geo-Electromagnetism. Academic Press, New York.
Walker, G.G., Kawasaki, K.K., 1988. Observation of double sign reversals in transient electromagnetic central induction soundings. Geoexploration 25, 245–254.
Weidelt, P., 1982. Response characteristics of coincident loop transient electromagnetic systems. Geophysics 47, 1325–1330.